New Combined Liquid Crystalline Polymers from Polyaddition of Biphenol Diglycidyl Ether and Trimeric Esters

Bao-Quan Chen, Atsushi Kameyama, and Tadatomi Nishikubo*

Department of Applied Chemistry, Faculty of Engineering, Kanagawa University, Rokkakubashi, Kanagawa-ku, Yokohama, 221-8686 Japan

Received March 8, 1999; Revised Manuscript Received July 9, 1999

ABSTRACT: Six trimers with biphenyl mesogenic groups and polymethylene spacers were synthesized. From these trimers and biphenol diglycidyl ether (BPGE), a new series of combined liquid crystalline polymers (LCPs) with polyether backbone were synthesized by the polyaddition with quaternary phosphonium chloride as catalyst. The effects of flexible spacer length on the phase transition and mesomorphism of the resulting trimers and combined LCPs were studied using differential scanning calorimetry (DSC), polarizing optical microscopy (POM), and X-ray diffraction. The trimers with 1,3-propylene and 1,4-butylene spacers were absent of mesophase, and the trimers with odd-numbered spacers, 1,5-pentylene and 1,7-heptylene, were nematic. In contrast, the trimers with even-numbered spacers, 1,6-hexylene and 1,10-decylene, were smectic within very narrow temperature ranges. All the combined LCPs were thermotropically nematic, though the crystalline behavior was complex with varying side-chain spacer length. The combined LCPs with 3, 5, and 10 methylene units (n) of side-chain spacers were semicrystalline at room temperature while other polymers were glassy. The combined LCPs showed general odd−even effects of side-chain length on T_{CP} and isotropization entropy in which the polymers with even numbers of methylene units in side-chain spacer showed higher values.

Introduction

Combined liquid crystalline polymers (LCPs) consist of a main-chain liquid crystalline backbone and side-chain mesogenic groups separated from the backbone via flexible spacers (Scheme 1).

The mesogenic structural cores in the main chain and side chain can be either identical or completely different. Those reported so far include azobenzene,[1−3] biphenylene,[4−6] *p*-phenylene benzoate,[3,4,6] and azoxybenzene.[6,7] The main chains of combined LCPs are either rigid (a) or semirigid (b, c). The rigid main chains, like the backbone in linear rigid-rod main-chain LCPs, consist of a sequence of para-linked aromatics by an even-numbered function, typically an ester or just none. In the case of a semirigid main chain, the mesogenic moieties are separated by flexible spacers along the backbone.[1,2,9,10] The side-chain mesogens are linked to the backbone via flexible spacers such as the spacers in a semirigid backbone. The attachment points of the side chains can be on the main-chain mesogens (b)[3,4,7] or on the main-chain spacers (c)[1,2,8−10] in the case of a semirigid backbone. The terminal groups of the side-chain mesogenic moieties have many alternatives as employed in low molecular weight liquid crystals.[5,7]

Since the first combined LCPs was prepared by Reck and Ringsdorf,[2,11] there have been about a dozen studies[3−10] on the correlation between liquid crystalline behavior and structural variations as mentioned above. Overall, the mesophase temperature range is surprisingly broadened in combined LCPs relative to corresponding main-chain and side-chain LCPs, because of a synergistic stabilization of the LC phase between the main-chain and side-chain mesogenic units.[9,11] The strong synergistic effect gives us hope to modulate relevant properties of a combined LCPs with a large range of values. For example, it is possible to develop high-performance combined LCPs with melt processability by the combination of high-modulus main-chain LCPs with side-chain LCPs which show mesophases at wide temperature ranges. Such a combination presents a modification method of main-chain LCPs to obtain melt-processable materials while keeping the ultrahigh modulus and strength.

Scheme 1

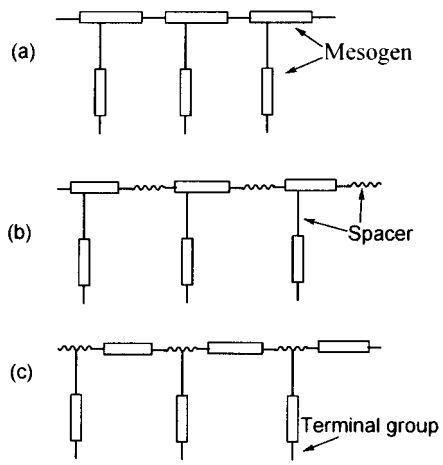

Although the effects of various structural variants of combined LCPs including the mesogenic structure, the spacer length, the stiffness of main chain, and the terminal group of the side-chain mesogen on the LC properties have been investigated in several groups,[1−15] we found from the literature so far that the polymerization method used to prepare combined LCPs was limited to polycondensation and the backbone type was polyester only. Other common polymerization methods, such as polyaddition and radical polymerization, have not been exploited yet in the synthesis of combined LCPs. This made us consider applying polyaddition between bis(epoxide) and "activated" diester to synthesize combined LCPs.

* To whom correspondence should be addressed.

10.1021/ma990348i CCC: $18.00
Published on Web 09/11/1999

Scheme 2

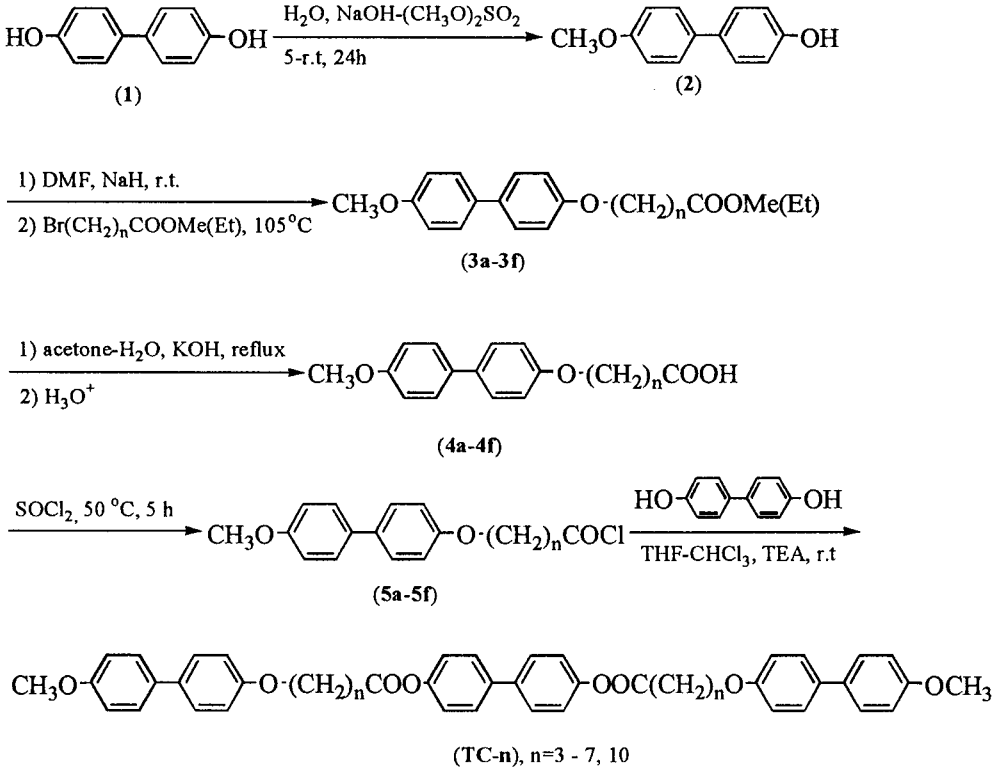

This paper describes a new synthetic route for combined LCPs and the significant odd−even effect of the side-chain spacer not only on the transition temperatures but also on the crystallinity of the resulting combined LCPs at below the mesophase temperatures. Moreover, the new polymers with polyether backbone structure are the first examples of such main-chain structure in the field of combined LCPs.

Results and Discussion

Synthesis of Monomers TC-*n*. The reactions to synthesize trimers (Scheme 2) are well-known. At first, biphenyl di(5-(*p*-methoxylbiphenoxyl)pentanate (TC-4) was synthesized. We found this compound was insoluble in common solvents. So, it was purified by careful boiling extractions of the precipitate from reaction by various solvents (see Experimental Section). The product was characterized by matrix-assisted laser desorption/ionization time-of-flight mass spectroscopy (MALDI TOF MS). MALDI TOF MS gave a very clean diagram. There was only one peak within the desired mass weight range. Elemental analysis gave reasonable agreement between the calculated and found elemental percentages. IR showed the strong C=O absorption at 1761 cm^{-1} without O−H (3400 cm^{-1}) and COOH (2400−3400 and 1700 cm^{-1}) absorption. Thereafter, other trimers, TC-*n* (n = 3, 5, 6, 7, 10), were synthesized, and it was found that the TC-5, TC-6, TC-7, and TC-10 were soluble in great amount of boiling $CHCl_3$ (ca. 1 g in 200−300 mL), and TC-3 had very low solubility in boiling acetone. However, the trimers were not soluble in other common solvents such as THF, CH_3CN, toluene, anisole, DMF, NMP, and DMSO up to 60 °C. Until now we have not found a solvent for TC-4 at medium temperature. TC-4 is the most insoluble compound in this series of trimers.

Polyaddition of BPGE with Trimers (TC-*n*). The polymerization is based on the addition reaction between epoxide and phenol ester functions.[17] This reaction is also catalyzed by quaternary ammonium or phosphonium salts effectively, as investigated in detail in our group.[18−22] In this work, the biphenyl diesters TC-*n* were reacted with BPGE to produce a series of combined LCPs (Scheme 3). Except for one polymerization (entry 2 in Table 1), tetraphenylphosphonium chloride (TPPC) was used as catalyst in polymerizations. The selection of TPPC as catalyst is due to its good stability below 200 °C and good catalytic activity

Scheme 3

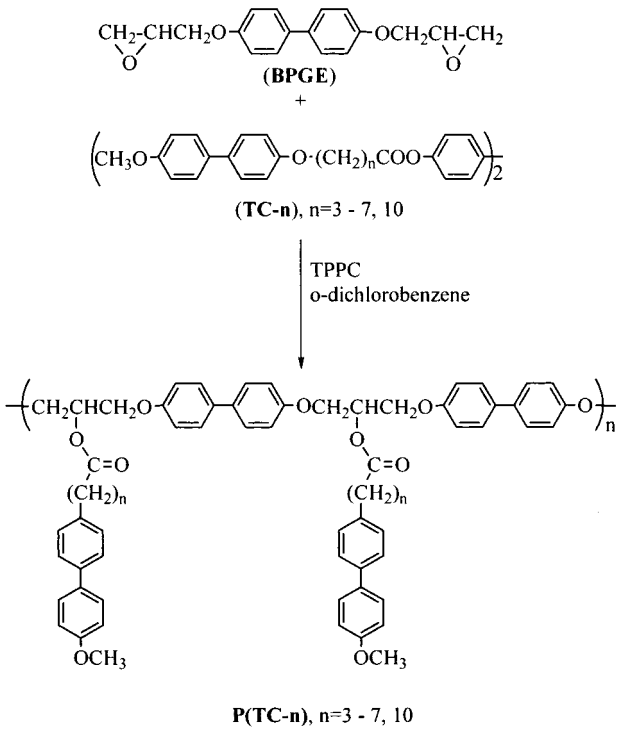

Table 1. Summary of the Polymerization Condition, Molecular Weight (M_n), and Molecular Distribution (M_w/M_n) for Combined LCPs P(TC-*n*)[a]

entry	LCPs	*n*	polymerization condition[b] temp, °C (time, h)	yield (%)	M_n[c] ($\times 10^{-4}$)	M_w/M_n[c]
1	P(TC-3)	3	145 (70) +160 (2) + 170 (1)	93	1.52	2.31
2	P(TC-4)	4	145 (96) +160 (2)[d]	98	3.65	1.88
3	P(TC-5)	5	145 (70) +160 (2) + 170 (1)	97	0.85	1.59
4	P(TC-6)	6	145 (70) +160 (2)	93	1.17	2.27
5	P(TC-7)	7	145 (70) +160 (2) + 170 (1)	94	1.57	1.97
6	P(TC-10)	10	145 (70) +160 (2)	91	1.77	5.41
7	LP(TC-5)	5	140 (72)	97	0.69	2.11
8	LP(TC-10)	10	140 (72)	85	0.42	2.18

[a] Polymerizations were carried out in 0.5 mmol scale in ampules with TPPC (5 mol %) in *o*-dichlorobeneze (0.5 mL). [b] The data in parentheses indicates the reaction times. [c] Measured by GPC in THF based on polystyrene standard. [d] With 8 mol % of TBPC catalyst.

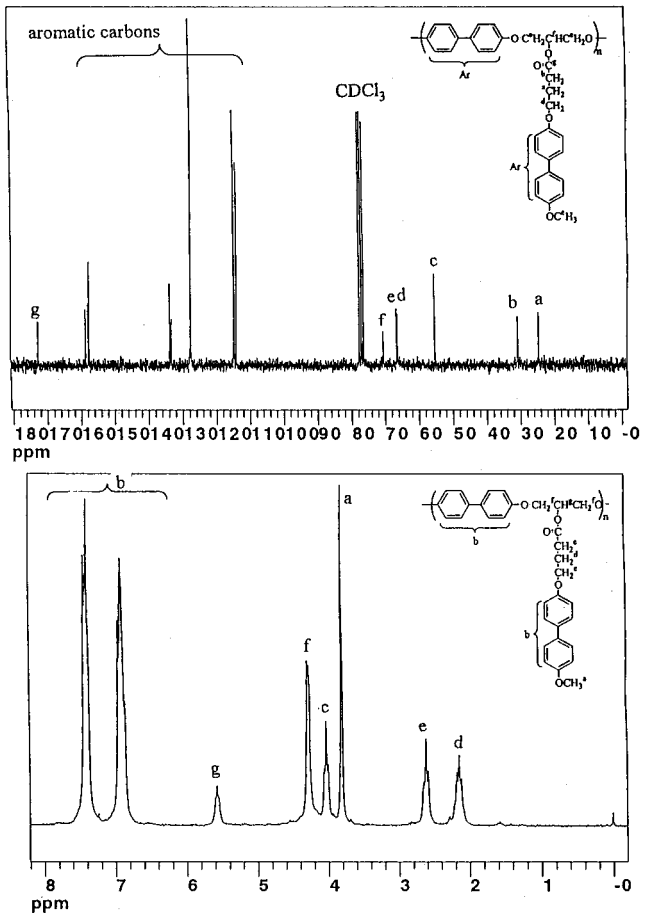

Figure 1. ^{1}H and ^{13}C NMR spectra of combined LCPs P(TC-3) from polyaddition of BPGE and TC-3.

observed in other polyadditions between epoxides and phenyl carboxylates. The polyadditions proceeded successively with 5 mol % of TPPC to provide polyethers. The high yields of the polymerizations and good solubility (in THF, $CHCl_3$) of the resulting polymers implied the occurrence of reaction between two monomers.

The structures of the polymers were characterized by ^{1}H, ^{13}C NMR, and IR spectra. For example, the ^{1}H and ^{13}C NMR spectra of P(TC-3) are shown in Figure 1 with peak assignments. Examining the ^{1}H NMR spectra of polyether P(TC-3) and BPGE (not shown here), the methylene peaks of the epoxy group around 2.8 ppm in the BPGE spectrum vanished completely in the polymer spectrum; meanwhile, a new peak at 5.57 ppm emerged, and the integral of the oxymethylene peaks increased though the peaks of the oxymethylene protons in the main chain overlapped with signals of oxymethylene in the side chain. The new peak at 5.57 ppm was assigned

Scheme 4

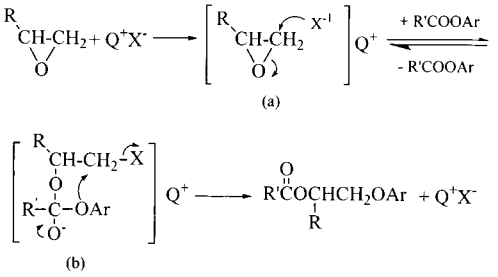

to the proton on the tertiary methyl in the main chain. The integral of this peak was one proton relative to that of middle methylene in side-chain spacer. The integral of oxymethylene peaks is nine protons based on the same standard.

The clean ^{13}C NMR of P(TC-3) showed six peaks of aliphatic carbons at high field and 11 peaks of aromatic peaks and one peak of C═O at low field. This sufficiently confirmed that the reaction proceeded regioselectively to give the polyether as shown in Scheme 3.

In IR spectra, it was found that the peak of C═O at 1761 cm^{-1} in TC-3 shifted to 1738 cm^{-1} in polymer P(TC-3). This red shift was attributed to the different electronic effect (E) between aliphatic ester and phenol ester. This result also suggests that the reaction occurred between the phenol ester and epoxy function.

The mechanism of the polyaddition is proposed in Scheme 4. At first, the quaternary cation combined with epoxy oxygen very fast. This combination polarized the C−O bonds of epoxy group and subsequently enhanced the epoxy reactivity (species a). Then, the epoxy oxygen attacks the carbonyl function on the carbon atom to form an sp^4 carbon (species b) with release of strain energy of epoxy function. At last, the phenol group transfers to the less-congested methylene of epoxy as shown by arrows in species b to afford the product, an aliphatic ester. The result is an insertion of an oxyethylene into the C−O bond of the ester.

The number-average molecular weights (M_n) and the molecular weight dispersities (M_w/M_n) of P(TC-*n*)s were measured by GPC using polystyrene as a standard. In Table 2, the polymerizations ended at high temperature (160 °C for 2 h and/or 170 °C for 1 h) gave polyethers with a reasonably high M_n while the polymerizations without raising to higher temperature at the last stage gave polyethers with a relatively low M_n (Table 1, entry 7, 8) at 140 °C for 72 h. Though the temperature rise was relatively small, this enhancement in the temperature improved the M_n by several times.

Liquid Crystalline Properties of Trimers TC-*n*. The trimers TC-*n* are a series of trimers with symmetric

Table 2. Transition Temperatures (°C), Enthropy Changes, and Entropy Changes of trimers TC-*n*[a]

trimer	*n*	cr		sm	n		iso	ΔH_1, kJ/mol	ΔS_1, J/(mol K)	ΔH_2, kJ/mol	ΔS_2, J/(mol K)
TC-3	3	×				247.9	×			102.6	196.9
TC-4	4	×	131.0[b]			230.2	×	4.4[c]	11.0	118.0	233.9
TC-5	5	×	208.3		×	267.1	×	70.9	147.2	17.8	33.0
TC-6	6	×	201.2	×		210.0	×			94.2	195.9[d]
TC-7	7	×	200.3		×	233.9	×	71.1	150.0	17.0	3.6
TC-10	10	×	182.0	×		189.6	×			106.6	230.3[d]

[a] cr, crystalline; sm, smectic; n, nematic, and iso, isotropic phases. ΔH_1, ΔH_2 are transition enthropy changes of crystal to nematic transition and isotropization, and ΔS_1, ΔS_2 are transition entropy changes of crystal to nematic transition and isotropization, respectively. The × symbol in the column means the presence of the corresponding phase. [b] Crystal−crystal transition. [c] The ΔH and ΔS of crystal−crystal transition. [d] The ΔH and ΔS of overlapping melting and clearing transition.

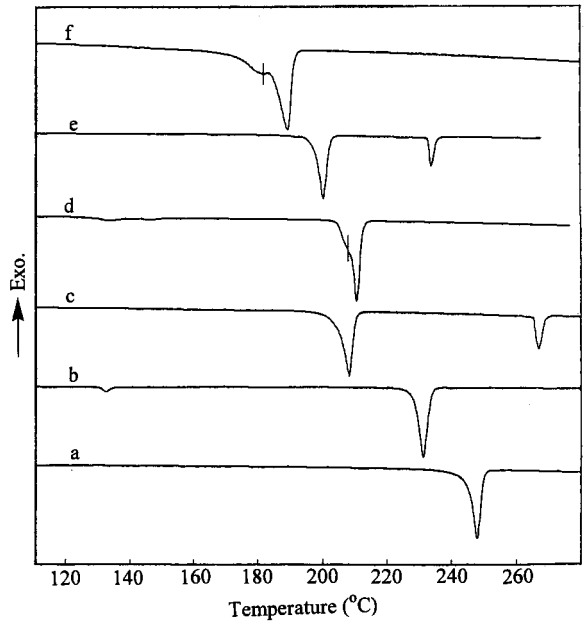

Figure 2. DSC traces of trimers TC-*n* of second heating scans at a rate of 5 °C/min under nitrogen atmosphere: a, TC-3; b, TC-4; c, TC-5; d, TC-6; e, TC-7; f, TC-10.

structure, composed of three mesogenic units and two flexible spacers. The phase transition temperatures measured by DSC were summarized in Table 2. The assignment of liquid crystalline phases was based on their optical textures and DSC patterns. The TC-3 had no mesophase transitions except an isotropization transition at elevated temperatures as shown on the DSC trace (Figure 2). TC-4 showed a solid−solid transition at 131 °C with low entropy change and an isotropization peak at 230.2 °C. TC-5 and TC-7 with odd numbers of methylene units in spacer showed mesophases. The nematic nature of these mesophases was easily confirmed by the observation of the unique texture of the nematic phase, i.e., nematic droplet texture (Figure 3, a) near clearing point (T_{cp}) and threaded texture (Figure 2b). The isotropization entropies (ΔS) of TC-5 and TC-7 were considerably high, even the ΔS_2 values by 3 times, corresponding to the ΔS of each mesogen group, were also rather high comparing with general nematic monomeric liquid crystals.

In contrast to TC-5 and TC-7, TC-6 and TC-10 with even numbers of methylene units in spacers exhibited a smectic phase at relatively narrow temperature ranges. On POM, a clear smectic texture was observed (Figure 3c) which is much different from the crystalline texture (Figure 4d) at low temperature.

It should be noted that the T_{cp} of TC-5 was far higher than that of any others. This can be attributed tentatively to the parity in length between mesogenic units (*p*,*p*′-biphenylene) and spacer (pentamethylene), as analyzed by Koltzenberg et al.[23] The identical parity between spacer and mesogen might offer an exceptionally tight packing and, hence, an increase of mesophase stability.

So, TC-*n* ($n = 3, 4$) with short spacers were non-liquid-crystalline. TC-*n* ($n > 5$) with long spacers were mesogenic and showed different mesophases between TC-*n* with odd and even numbers of methylene in spacer.

Recently, Imrie and Luckhurst reported a series of trimers,[16] 4,4′-bis[ω-(4-cyanobiphenyl-4′-yloxy)alkoxy]-biphenyls, with spacers varying from 3 to 12 methylene units. The trimers in that paper showed very regular behavior, enantiotropic nematic phases for all the trimers, and, in addition, monotropic smectic A phases with spacers containing from 4 to 11 methylene units. The orientational ordering of the nematic phase in those trimers was significantly higher than the corresponding dimers and monomers. However, in our case, the trimers with odd and even number of methylene units in spacers showed considerably different temperature ranges of nematic phases. It seems that the ester linkages bridging the spacers and rodlike cores had an essential effect on the stability of the mesophases.

Liquid Crystalline Properties of Combined Liquid Crystalline Polyethers. The thermal properties of P(TC-*n*)s are summarized in Table 3. Although the transition behavior changed in a complex manner with varying length of side-chain spacers, all the P(TC-*n*)s were thermotropically nematic LCPs as commonly combined LCPs with main-chain spacers and side-chain spacers in different length favored the formation of a nematic phase.[9−12]

Polymers P(TC-3) and P(TC-10) were semicrystalline at room temperature. They transformed from semicrystalline solids directly into liquid-crystalline phases at 132.8 and 104.2 °C, respectively. The mesophase was nematic with clearing temperatures at 146.2 °C for P(TC-3) and 123.3 °C for P(TC-10), respectively. The nematic phases showed typical fine schlieren textures (see Figure 4a for an example) on POM as observed in general high-M_n LCPs.[25] The grainy speckles disappeared gradually with annealing to form a homeotropic texture (Figure 4b). With further cooling, this alignment was destroyed with the reformation of a grainy polydomain texture identical to the previous texture. Although the P(TC-3) and P(TC-10) showed the same mesophase, the conformations of spacer chains were different to fit both side-chain and main-chain mesogens parallel to each other for the nematic orientation.

The P(TC-*n*)s with $n = 4, 6, 7$ were amorphous at room temperature as confirmed by DSC (Figure 5), POM, and X-ray diffraction. For example, in P(TC-6), there were a steplike transition at around 63 °C on the DSC heating trace. The transition was ascribed to a

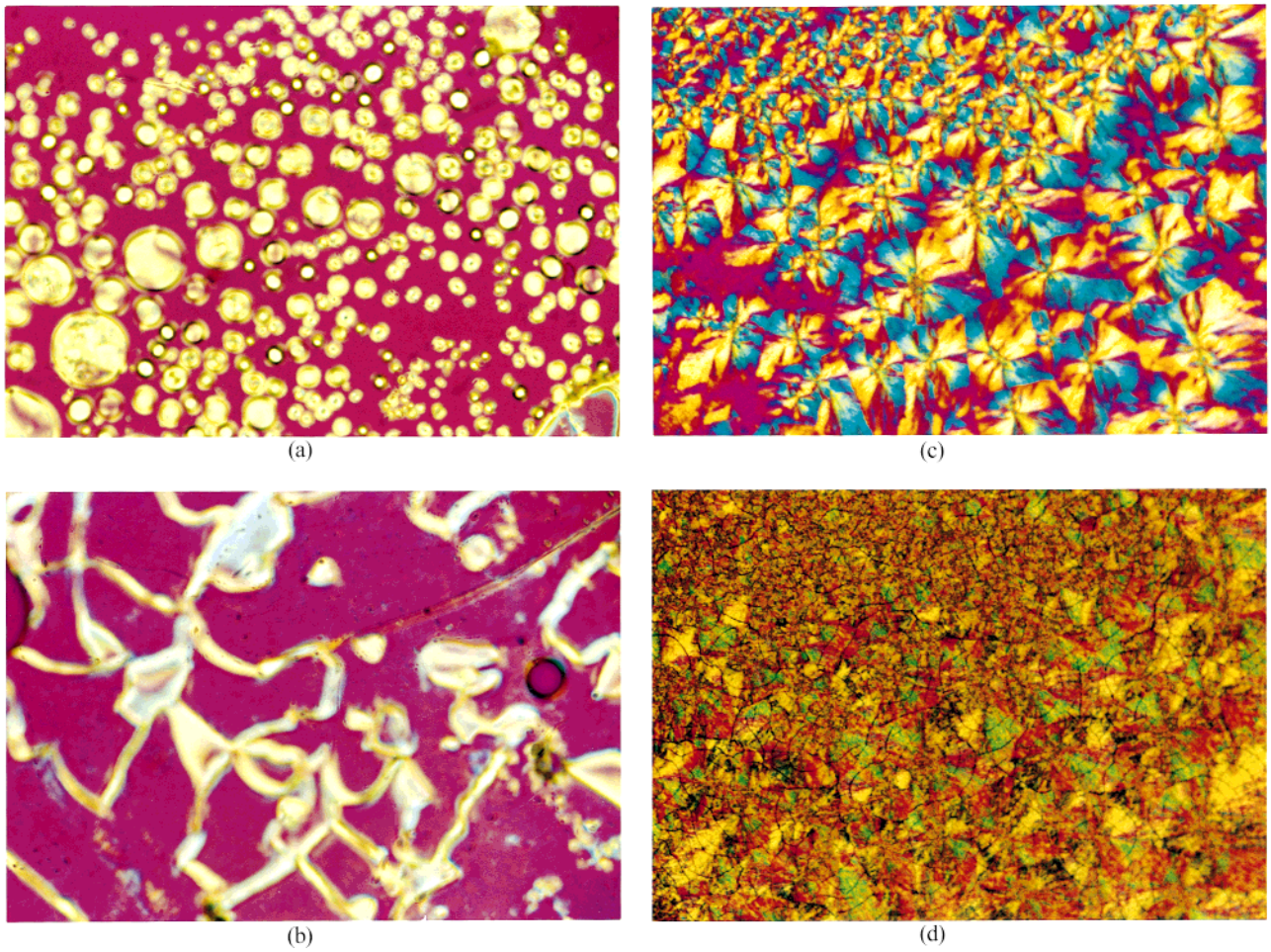

Figure 3. Photos of mesophase texture taken on POM: (a) droplets with extinction crosses at 261.5 °C on cooling isotropic liquid of **TC-5** at 2 °C/min; (b) typical threaded texture of TC-5 (same area as a) cooling to 200 °C; (c) focal-conic fan texture of smectic phase of TC-10 heating to 188 °C; (d) crystalline texture at room temperature.

Table 3. Transition Temperatures, Enthropy Changes, and Entropy Changes of Combined LCPs P(TC-*n*)[a]

LCPs	*n*	cr		g		n		iso	ΔH_1, kJ/mol	ΔS_1, J/(mol K)	ΔH_2, kJ/mol	ΔS_2, J/(mol K)
P(TC-3)	3	×	132.8[b]			×	146.2	×	9.23	22.7	0.62	1.48
P(TC-4)	4			×	73.1[c]	×	156.1	×			1.29	3.02
P(TC-5)	5	×	73.3[c,d]	×	99.5[b]	×	127.3	×	3.33[d]	8.97	0.66	1.64
P(TC-6)	6			×	62.7[c]	×	135.5	×			2.10	5.13
P(TC-7)	7			×	55.1[c]	×	118.0	×			1.38	3.53
P(TC-10)	10	×	104.2[b]			×	123.3	×	15.4	40.5	3.04	7.76
LP(TC-5)	5	×	69.9[c,d]	×	98.2	×	130.3	×	3.37[d]	9.07	0.80	1.97
LP(TC-10)	10	×	106.2[b]			×	118.3	×	11.3	29.9	2.47	6.23

[a] cr, crystalline; am, amorphous; n, nematic, and iso, isotropic phases. ΔH_1, ΔH_2 are transition enthropy changes of crystal to nematic transition and isotropization, and ΔS_1, ΔS_2 are transition entropy changes of crystal to nematic transition and isotropization, respectively. The × symbol in the column means the presence of the corresponding phase. [b] Crystal to nematic transition temperature. [c] Glass transition temperature. [d] Depending on quenching rate.

glass transition. Optical microscopic observation indicated that, below T_g, the polymer had not any birefringence. Wide-angle X-ray diffraction of P(TC-6) sample prepared by slowly cooling the melt to room temperature showed no reflections but a defused reflection at around $2\theta = 16.5°$. The endothermic peak at 135.5 °C corresponded to mesophase−isotropic transitions. The mesophase was a nematic phase according to X-ray diffraction and optical observation. The thermal behavior of P(TC-4) and P(TC-7) was similar to that of P(TC-6), as confirmed by POM and DSC.

The P(TC-*n*) ($n = 4, 6, 7$) on a glass plate were highly viscous and cloudy fluids from which fiber could be easily drawn out at temperatures between T_g and T_{CP}. This indicated that these polymers (P(TC-*n*), $n = 4, 6, 7$) transformed directly from an amorphous state into the mesophase, and the spacer with mediate length in these combined LCPs suppressed the regular packing of mesogenic groups for crystallization as the temperature dropped. The mesophase textures of P(TC-4), P(TC-6), and P(TC-7) showed the same features as polymer P(TC-10) and were assigned to the nematic phase without problem. The small entropy changes (ΔS) of isotropization of these polymers also supported these determinations.

The DSC curve of P(TC-5) (Figure 5, curve c) showed four transitions at 73.3, 84.3, 99.5, and 127.3 °C on a second heating scan. These peaks could be repeated on subsequent scans of the fast-quenched sample. The step transition at ca. 73.3 °C was attributed to a glass

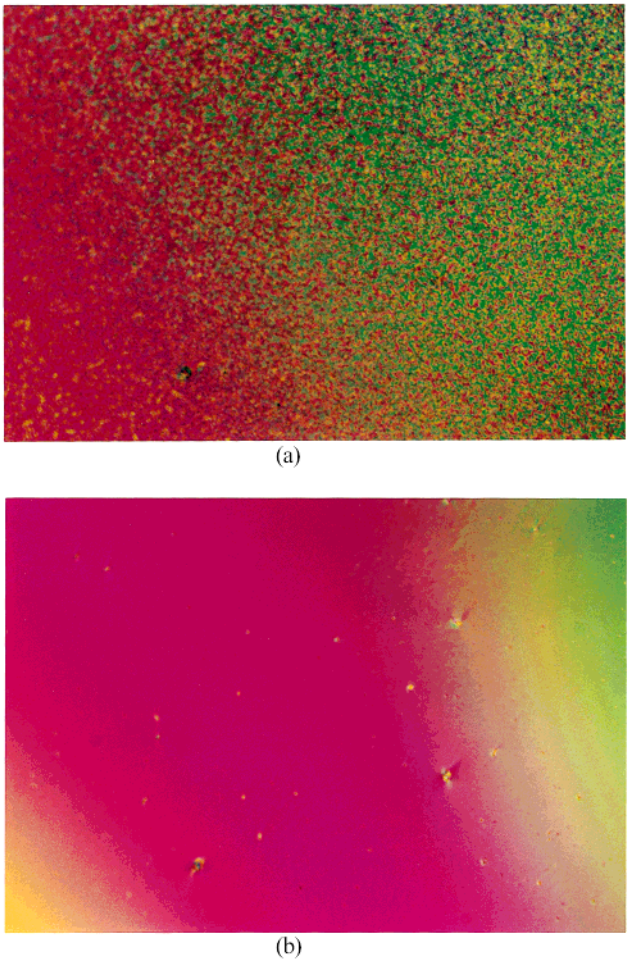

Figure 4. (a) Grainy texture of P(TC-10) cooling to 116 °C from isotropic liquid and (b) homeotropic texture on annealing the sample at 116 °C for 40 min (same area as a).

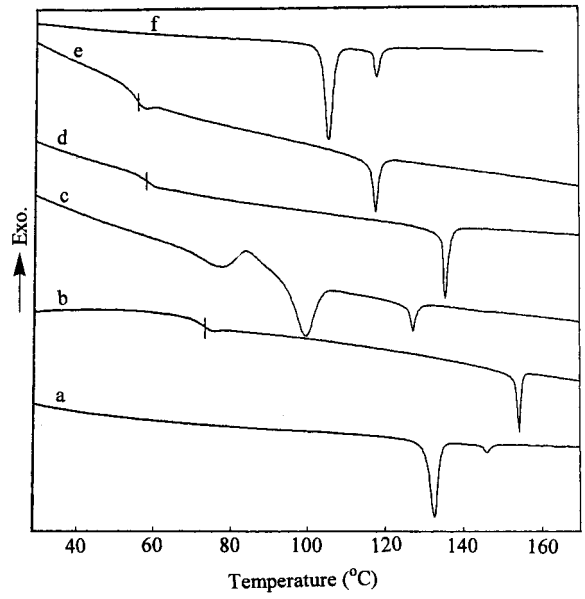

Figure 5. DSC traces of P(TC-*n*) during the second heating cycle at a rate of 5 °C/min under nitrogen atmosphere: a, P(TC-3); b, P(TC-4); c, P(TC-5); d, P(TC-6); e, P(TC-7); f, P(TC-10).

transition which was connected to an exothermic premelt−recrystallization transition (84.3 °C). The intermediate endothermic peak at 99.5 °C represented a crystal−mesophase transition. The highest temperature peak represented the T_{CP}. The mesophase between 99.5 and 127.3 °C had nematic nature on POM. The complicated polyphase of P(TC-5) was due to the high tendency attributed to the identical length of spacer and mesogen.

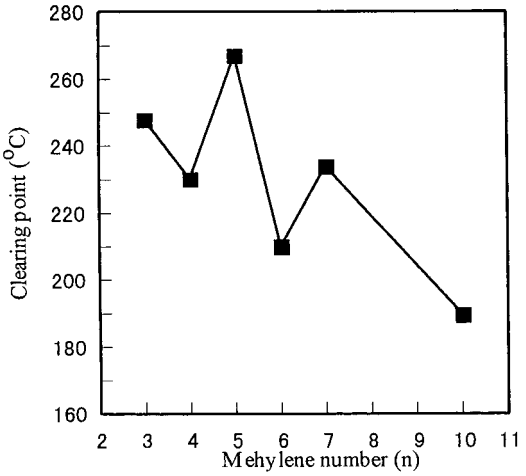

Figure 6. Plot of clearing temperature (T_{CP}) versus the number of methylene units of flexible side-chain spacer of combined LCPs P(TC-*n*).

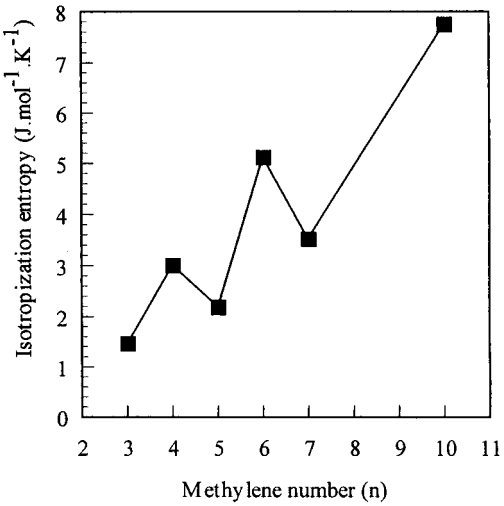

Figure 7. Plot of isotropization entropy change against the number of methylene units of flexible side-chain spacer.

In this series of combined LCPs, the dependence of isotropization temperature and T_g on side-chain spacer length could be plotted in Figure 6. The isotropization temperature decreased with growing spacer length and showed a considerably high odd−even effect related to the methylene numbers of side-chain spacers. The LCPs with even numbers of methylene in side-chain spacer had relatively high T_{CP}. Generally, both the mesophase−isotropic transition temperature and the associated entropy change should show the same odd−even effect. The ΔS_2 versus methylene numbers in side-chain spacer was plotted in Figure 7. The ΔS of clearing transition also displayed a pronounced odd−even fluctuation with the even-numbered polymers exhibiting the higher transition temperatures. The ΔS of isotropization increased in tendency by increasing the length of the flexible lateral spacer, with P(TC-10) having the largest ΔS value of 5.4 J mol^{-1} K^{-1}, implying that orientation order in nematic phase increased with increasing side-chain spacer length. This means that the nematic orientational ordering increase with increase of the side-

chain spacer length. This behavior was similar to that of the side-chain LCPs.

The molecular weight also affected the phase transition temperatures. This was seen in LP(TC-10) and P(TC-10). The M_n of LP(TC-10) was ca. one-fourth that of P(TC-10); although they exhibited the same thermal behavior, the transition temperatures had a little difference (ca. 5 °C).

Conclusion

As described above, a series of trimers were synthesized at first. The trimers showed an extraordinary odd−even effect of spacer length on mesomorphism opposite to the reported rule in the literature. The trimers with short spacers did not exhibit mesophases. Trimer TC-5 with pentamethylene as spacer showed the broadest nematic phase. TC-6 and TC-10 showed narrow smectic phases. Then, we presented an alternative method for the synthesis of combined LCPs with a new type of main-chain structure, polyether. These combined LCPs showed a very strong odd−even effect of side-chain spacer length on T_{CP} and isotropization entropy were very strong. With only one methylene unit, variation in side-chain spacer could result in completely different crystalline nature, different to that reported in the literature so far. The mediate spacers suppressed the crystallization in the combined LCPs.

Experimental Section

Materials. THF, $CHCl_3$, DMF, and *o*-dichlorobenzene used in the reactions were dried and purified in the usual ways. Tetrabutylphosphonium chloride (TBPC) and tetraphenylphosphonium chloride (TPPC) (from TCI) were used after being dried in vocuum at 90 °C for 4 h. Methyl (or ethyl) ω-bromoalkylcarboxylates were dried over 4 Å MS. Silica gel used for flash chromatography was Wakogel-200 (100−200 mesh). Other materials were used as received.

Measurement. TLC was performed on Kiesegel 60 F254 plates (Merk). Infrared (IR) spectra were measured on a JASCO model IR-700 spectrometer. The ^{1}H and ^{13}C NMR spectra were recorded on JEOL models JNM FX-200 (200 MHz) instruments in $CDCl_3$ using Me_4Si (TMS) as an internal standard unless otherwise specified. The molecular weights of polymers were estimated by gel permeation chromatography (GPC) on a TOSOH model HLC-8120 GPC equipped with UV and reflective index detectors using TSK gel columns (eluent: THF, calibrated with polystyrene standards). MALDI TOF MS were performed on a Kompact MALDI IV mass spectrometer (Shimadzu/Kratos). A 0.5 μL aliquot of solutions of matrix (dithranol) and samples (20:1) in acetone or $CHCl_3$ was dropped on a sample holder and air-dried. The spectra were recorded in the reflection mode with 100 gains using 20 kV accelerating voltage with detection of positive ions. DSC thermograms were run on a DSC 120 unit of thermal analysis station (SSC 5200, Seiko Instruments Inc.) at scan rate of 5 °C under a nitrogen atmosphere. The second heating scans were used to read transition temperatures. A hot-stage (Mettler FP84) equipped with a programmable temperature controller and a microscope (Olympus BH-2) with a camera connected to an autoexposure control unit (Olympus) were used to observe mesophase texture and to take pictures under cross-polarized light with a 530 nm light filter.

Synthesis. Biphenol diglycidyl ether (BPGE) was synthesized by a standard procedure[25] in which the biphenol reacted with excess of epichlorohydrin and then with K_2CO_3 in the presence of tetrabutylammonium chloride catalyst in DMF.

4-Methoxy-4′-hydroxybiphenyl (**2**) was synthesized after a literature procedure.[26] Ethyl (methyl) ω-[(4-methoxybiphen-4′-yl)-oxy]alkyl-1-carboxylates were synthesized according to a modified procedure of synthesizing ethyl-5-(4-phenylphenoxy)valerate and 5-[4-(butoxybiphenyl)oxy]hexanoic acid.[27,28] A general procedure was as follows. A 20 mmol aliquot of 4-methoxy-4′-hydroxybiphenyl was dissolved in dry DMF under nitrogen atmosphere. A 21 mmol aliquot of NaH (60% in oil) was added in portions at room temperature. Then, 20 mmol of ω-bromoalkyl carboxylate was added via a syringe and a rubber septa immediately. The system was moved to a 110 °C oil bath for an additional 3 h. Upon cooling, the mixture was partitioned between THF and water. The THF layer was washed by water, dried ($MgSO_4$), filtered, and evaporated to give crystals. Recrystallization in methanol gave white crystals. For example:

Ethyl 4-(4-methoxybiphenoxy)butanate (**3a**) was obtained in 94% yield; mp 92.4−93.2 °C. ^{1}H NMR ($CDCl_3$, δ): 1.26 (t, 3H, CH_3), 2.16 (m, 2H, CH_2), 2.53 (t, 2H, $CH_2C{=}O$), 3.83 (s, 3H, OCH_3), 4.03 (t, 2H, $ArOCH_2$), 4.15 (q, 2H, $COOCH_2$), 6.90−6.97 (q, 4H_{Ar}), 7.43−7.49 (q, 4H_{Ar}). IR (KBr, cm^{-1}): 3116, 2958 (C−H), 1736 (C=O), 1607, 1500 (C=C), 1273, 1247, 1179 (C−O−C), 824 (aromatic C−H, out-of-face).

ω-[(4-Methoxybiphen-4′-yl)-oxy]alkyl-1-carboxylic chlorides were prepared by the reactions of corresponding acids with excess $SOCl_2$ at 50−55 °C for 5 h. After removal of excess $SOCl_2$, the compounds were used for the next step immediately after preparations. For example, 4-(4-methoxybiphenoxy)-butanoic chloride (**5a**) has the following spectra data. ^{1}H NMR ($CDCl_3$, δ): 2.12−2.28 (m, 2H, CH_2), 3.15 (t, 2H, $CH_2C{=}O$), 3.84 (s, 3H, OCH_3), 4.04 (t, 2H, OCH_2), 6.89−7.00 (q, 4H_{Ar}), 7.42−7.54 (q, 4H_{Ar}). IR (KBr, cm^{-1}): 1800 (C=O), 1607, 1502 (C=C), 1275, 1251 (C−O−C), 822 (aromatic C−H, out-of-face), 748 (C−Cl).

4,4′-Biphenylbis[ω-(4-methoxybiphenyl-4′-oxy]alkyl 1-carboxylates (TC-*n*) were synthesized by the reactions of acid chlorides (6 mmol) with biphenol (2.4 mmol) in the presence of TEA at room temperature for 36 h. The reaction mixtures were filtered. The collected powders were washed on a Pyrex glass filter with THF (2 × 50 mL), acetone (2 × 100 mL), and $CHCl_3$ (2 × 50 mL), successively. The residues were further purified by different methods according to their solubility. For TC-3 (ca. 1.7 g), seven times of boiling extractions by $CHCl_3$ (500 mL), toluene (300 mL), toluene−$CHCl_3$ (300/50 mL), acetone (2 × 400 mL), THF (300 mL), and $CHCl_3$ (300 mL) were applied successively to remove impurities. For TC-4 (2.0 g), five times extraction by $CHCl_3$ (50 mL), THF (150 mL), acetone (200 mL), and $CHCl_3$ (2 × 200 mL) were carried out. Other trimers were extracted by heat THF and recrystallized in $CHCl_3$ three times. For example, TC-3 was obtained in 70% yield. MALDI TOF MS (acetone, $AgOOCCF_3$, *m*/*z*): Calcd for $C_{46}H_{42}O_8$: 722.83. Found: 830.17 ($M + Ag^+$). IR (KBr, cm^{-1}): 2935, 2911 (C−H), 1760 (C=O), 1608, 1498 (C=C), 1272, 1240, 1180 (C−O−C), 813 (aromatic C−H, out-of-face). Elemental Anal. Calcd for $C_{46}H_{42}O_8$: C, 76.44; H, 5.86. Found: C, 75.14, H, 5.82.

Polymerization. All the weighting operation was carried out in P_2O_5-dried glovebox (humidity <10%). A general procedure for polyaddition of BPGE with TC-*n* was as follows: To a 10 mL ampule was charged with TPPC (9.4 mg, 0.025 mmol). The ampule was moved to attach on Shlenk line for drying at 90 °C for 4 h. Then, trimer (0.5 mmol), BPGE (0.5 mmol), and *o*-dichlorobenzene (0.5 mL) were added. The ampule was degassed (four freeze−pump−thaw cycles), sealed, and then immersed in an oil bath set at certain temperature for polymerization. After the required time of reaction, the contents were precipitated into hexane (100 mL) and filtered. The collected polymer was further purified by twice precipitation from THF solution into methanol (100 mL). The collected polymer was dried at 60 °C in vacuum for 24 h before characterization. The yields of polymerizations are listed in Table 1. The spectra data for P(TC-3), as an example, is as follows.^{1}H NMR ($CDCl_3$, δ): 2.14 (2H, CH_2), 2.61 (2H, $CH_2C{=}O$), 3.80 (3H, OCH_3), 4.02 (2H, OCH_2), 4.27 (4H, OCH_2CHCH_2), 5.57 (1H, CHO), 6.91 (8H_{Ar}), 7.41 (8H_{Ar}). ^{13}C NMR ($CDCl_3$, δ): 24.56, 30.76, 55.18, 66.25, 66.53, 70.42 (aliphatic C), 114.06, 114.67, 114.85, 127.54, 127.66, 133.25, 133.38, 133.77, 157.49, 157.80, 158.59 (aromatic C), 172.55 (C=O). IR (film, cm^{-1}): 3036, 2936 (C−H), 1738 (C=O), 1607, 1499 (C=C), 1242, 1174

(C−O−C), 821 (aromatic C−H, out-of-face). Elemental Anal. Calcd for $(C_{32}H_{30}O_6)_n$: C, 75.28; H, 5.92. Found: C, 74.72, H, 5.74.

Acknowledgment. This work was supported by the Original Industrial Technology R & D Promotion Program (No. 8A-045-1) from the New Energy and Industrial Technology Development Organization (NEDO) of Japan, which is gratefully acknowledged.

References and Notes

(1) Voigt-Martin, I. G.; Durst, H.; Reck, B.; Ringsdorf, H. *Macromolecules* **1988**, *21*, 1620−1626.
(2) Reck, B.; Ringsdorf, H. *Makromol. Chem. Rapid Commun.* **1985**, *6*, 291.
(3) Piao, X. L.; Kim, J.-S.; Yun, Y.-K.; Jin, J.-I.; Hong, S.-K. *Macromolecules* **1997**, *30*, 2294.
(4) Reck, B.; Ringsdorf, H. *Makromol. Chem.* **1989**, *190*, 2511.
(5) Kapitza, H.; Zentel, R. *Makromol. Chem.* **1991**, *192*, 1859.
(6) Pakula, T.; Zentel, R. *Makromol. Chem.* **1991**, *192*, 2401.
(7) Reck, B.; Ringsdorf, H. *Makromol. Chem. Rapid Commun.* **1986**, *7*, 389.
(8) Ge, J. J.; Zhang, A.; McCreight, K. W.; Ho, R.-M.; Wang, S.-Y.; Jin, X.; Harris, F. W.; Cheng, S. Z. D. *Macromolecules* **1997**, *30*, 6498.
(9) Endres, B. W.; Ebert, M.; Wendorff, J. H.; Reck, B.; Ringsdorf, H. *Liq. Cryst.* **1990**, *7*, 217.
(10) Diele, S.; Naumann, M.; Kuschel, F.; Reck, B.; Ringsdorf, H. *Liq. Cryst.* **1990**, *7*, 721.
(11) Zentel, R.; Brehmer, M. *Acta Polym.* **1996**, *47*, 141.
(12) Zentel, R. In *Handbook of Liquid Crystals*; Demus, D., Goodby, J., Gray, G. W., Spiess, H.-W., Vill, V., Eds.; Wiley-VCH: Weinheim-New York, 1998; Vol. 3, Chapter I, p 52.
(13) Zentel, R.; Reckertand, G.; Reck, B. *Liq. Cryst.* **1987**, *2*, 83.
(14) Kapita, H.; Zentel, R. *Makromol. Chem.* **1988**, *189*, 1793.
(15) Cooray, N. F.; Fujimoto, H.; Kakimoto, M.; Imai, Y. *Macromolecules* **1997**, *30*, 3169.
(16) Imrie, C. T.; Luckhurst, G. R. *J. Mater. Chem.* **1998**, *8*, 1339.
(17) Funahashi, K. *Bull. Chem. Soc. Jpn.* **1979**, *52*, 1488.
(18) Nishikubo, T.; Kameyama, A. *Prog. Polym. Sci.* **1993**, *18*, 963.
(19) Nishikubo, T.; Iizawa, T.; Saito, Y. *J. Polym. Sci., Polym. Chem.* **1983**, *21*, 2291.
(20) Nishikubo, T.; Iizawa, T.; Takahashi, E.; Nono, F. *Macromolecules* **1985**, *18*, 2131.
(21) Nishikubo, T.; Iizawa, T.; Takahashi, E.; Nono, F. *Polym. J.* **1985**, *16*, 371.
(22) Sato, K.; Nishikubo, T. *Nippon Kagaku Kaishi* **1991**, 1514.
(23) Koltzenberg, S.; Wolff, D.; Spring, J.; Nyuken, O. *J. Polym. Sci., Polym. Chem.* **1998**, *36*, 2669.
(24) Aldermann, N. J.; Mackley, M. R. *Faraday Discuss. Chem. Soc.* **1985**, *79*, 149.
(25) Brennan, D. J.; White, J. E.; Brown, C. N. *Macromolecules* **1998**, *31*, 8281 and references therein.
(26) Viney, C.; Mitchell, G. R.; Windle, A. H. *Mol. Cryst. Liq. Cryst.* **1985**, *129*, 5.
(27) Rodriguez-Parada, J. M.; Percec, V. *J. Polym. Sci., Polym. Chem.* **1986**, *24*, 1363.
(28) Bazuin, C. G.; Brandy, F. A.; Eve, T. M.; Plante, M. *Makromol. Symp.* **1994**, *84*, 183.

MA990348I